Synthesis and characterization of a new Azo dye and study of its adsorption mechanism on graphene oxide nanoparticles

Abeer Hussein Ali*, *Liqaa* Hussein Alwan, and *Diana* AbdAlkreem Al-Rifaie

Department of Applied Chemistry, Samarra University, Samarra, Iraq

Abstract. In this study, a novel azo dye was successfully synthesized, and its molecular structure was confirmed using comprehensive spectroscopic analyses. The adsorption performance of the dye onto graphene oxide (GO) nanoparticles was systematically investigated to evaluate its potential as an effective nano-adsorbent for pollutant removal. Thermodynamic analysis revealed that the adsorption process was exothermic, indicating stable interactions between the dye molecules and the graphene oxide surface. Kinetic modeling demonstrated that the adsorption behavior followed a pseudo-second model, suggesting that chemisorption is the dominant mechanism controlling the adsorption rate. Overall, the results highlight the promising applications of graphene oxide nanoparticles as effective materials for removing dyes and organic pollutants from aqueous environments.

1 Introduction

The synthetic dye category of azo dyes holds significant importance because they contain one or more azo groups (–N=N–) that link to aromatic systems. The extensive range of structures and deep colors in azo dyes makes them useful for textile and polymer manufacturing as well as biomedical applications [1]. Scientists use molecular components of these compounds to perform exact chemical transformations, which result in dyes with specific functional characteristics. The production of these compounds involves traditional diazotization methods together with advanced Gewald reaction techniques, which create heterocyclic azo dyes and expand their derivative applications [2]. The combination of pyrazole nuclei in heterocyclic azo dyes produces compounds that show better physical and chemical properties. The fastness properties of leather substrates become better when pyrazole-based azo dyes are made through diazotization of 4-aminoacetanilide followed by condensation with substituted hydrazones, which results in dyes that show λ_max values between 388 and 401 nm [3]. The stability and functional properties of these dyes depend on their structural behavior through tautomerism and cis–trans isomerism, which respond to environmental conditions [4]. The industrial benefits of azo dyes, including their strong coloration and chemical stability and affordable production costs, do not outweigh the major environmental problems they create. Textile wastewater contains persistent dyes, which

* Corresponding author: eduhm230039@uosamarra.edu.iq

block light transmission and damage photosynthesis and resist standard wastewater treatment techniques [5 New sustainable treatment methods need to be implemented because environmental regulations continue to grow stronger. The process of bioremediation shows promising results because various microorganisms, including bacteria, fungi, and algae, produce enzymes that break down azo bonds through reduction. The combination of aerobic and anaerobic treatment systems with microbial consortia immobilized in these systems achieves superior results for dye color removal and substance breakdown [6]. The treatment of dye-contaminated wastewater now uses photodegradation with advanced nanomaterials as an environmentally friendly biological method. Metal oxide and ferrite-based materials show photocatalytic properties, which enable them to break down azo compounds through light activation for industrial wastewater treatment [5, 7]. The biomedical field now uses azo dyes and their metal complexes for research purposes. The combination of azo dyes with transition metals Cu (II), Fe (III), and Zn (II) produces compounds that demonstrate superior antimicrobial activity because of their enhanced lipophilicity and redox properties [1]. However, the textile, leather, plastics, cosmetics, and food manufacturing industries face ongoing difficulties because of azo dye contamination in their production processes. The combination of strong aromatic structures and high-water solubility and resistance to chemical and biological breakdown makes azo dyes persistent in water bodies, which creates potential health threats for humans and aquatic species [4, 5]. The treatment of azo dyes through conventional methods such as adsorption and oxidation and filtration and coagulation faces multiple challenges because of pH sensitivity and dye concentration and temperature variations, which result in high operational expenses and potential secondary pollution [8]. Research shows that azo dyes in functional systems become more reactive when scientists add nanostructured carbon materials, which include graphene derivatives, to their design. The high number of oxygen-containing functional groups in graphene oxide (GO), along with its strong aromatic and heterocyclic dye-binding properties, makes it suitable for developing advanced dye-nanomaterial hybrid systems [7,8] The research on bioremediation and photocatalysis follows green chemistry and circular economy principles to develop sustainable resource recovery systems through combined composting and enhanced wastewater treatment methods [6,7]. The two-dimensional carbon-based nanomaterial nano-graphene oxide (n-GO) provides outstanding environmental benefits because it disperses well in water, contains many reactive sites, and shows excellent hydrophilic properties [9]. The production of n-GO requires modifications to Hummer's method and electrochemical oxidation and alternative chemical methods. The combination of n-GO with metal oxides and metal–organic frameworks (MOFs) lead to better adsorption and catalytic activity in hybrid materials. The combination of CuO with GO and HKUST-1 with GO produces materials that show enhanced mechanical properties and superior pollutant elimination capabilities [10,11]. The CuO/GO nanomotors achieve more than 90% methylene blue removal through their self-propelled movement and their ability to produce reactive oxygen species during a 120-minute treatment period [12]. The HKUST-1/GO hybrid material shows excellent cationic dye adsorption capabilities through pseudo-second-order kinetics and both Freundlich and Langmuir isotherm models [13]. The green preparation of n-GO–CuO composites through plant extract processing creates environmentally friendly materials that exhibit antimicrobial properties [14] The development of wastewater treatment systems needs adsorption kinetic studies to determine which factors control the rate of process. The pseudo-first-order, pseudo-second-order, intraparticle diffusion, and Elovich equations serve as essential tools to study adsorption mechanisms. The development of adsorption-based systems needs exact kinetic modeling to boost operational performance and create sustainable industrial operations [15].

2 Experimental section

The characterization analysis of the synthesized samples was conducted using a range of analytical instruments. UV–Vis spectra were recorded using a PerkinElmer Lambda 35 UV–Vis spectrophotometer. Fourier transform infrared (FTIR) analysis was performed using a Shimadzu 8400S spectrometer with potassium bromide granules in the 4000–4000 cm^{-1} range. The crystal structure of the materials was investigated by X-ray diffraction (XRD) using a Hitachi S-4800 diffractometer (Japan). Surface morphology and microscopic properties were studied using a field emission scanning electron microscope (FE-SEM, MIRA3, TESCAN, Iran) operating at an accelerating voltage of 15 kV.

2.1 Chemical and materials

2-amino-5-bromo 1,3,4-thiadiazo, l Graphite, Potassium permanganate, Vanillin, Sodium nitrate, Sodium nitrite, Hydrogen peroxide dye (from Sigma-Aldrich (UK).

2.2 Procedure

The textile, leather, and paper industries face industrial dye pollution as their main environmental challenge because azo dyes remain stable in water and resist biological breakdown. The stable chemical structure of azo dyes together with their non-biodegradable nature causes these substances to stay in water bodies and soil environments, which threatens both environmental systems and human wellness. The solution to these contaminants needs researchers to create efficient wastewater treatment systems that operate sustainably.

The exceptional surface area of graphene oxide (GO) combined with its numerous oxygen-based functional groups makes it an effective nanomaterial for dye removal. The specific structure of GO enables it to adsorb organic pollutants, including azo dyes, through strong electrostatic forces and hydrogen bonds and aromatic ring interactions. The production of GO follows a simple method that allows researchers to incorporate additional materials for improving its performance through composite material development. The adsorption of azo dyes onto GO surfaces happens through three main mechanisms, which include electrostatic forces, hydrogen bonding, and π–π stacking between dye aromatic rings and GO conjugated domains.

The properties of GO-based nanomaterials show promise for using them as environmentally friendly adsorbents to remove azo dyes from wastewater

2.3 Preparation of nano graphene oxide

A 600 mL reaction flask was placed in an ice bath, and 46 mL of concentrated sulfuric acid (H_2SO_4) was carefully added with continuous magnetic stirring at 0°C. Sodium nitrate ($NaNO_3$, 0.017 mol, 1.45 g) was then added gradually over 15 minutes with continuous stirring. Next, graphite (1 g) was added over 10 minutes. Potassium permanganate ($KMnO_4$, 0.03 mol, 4.74 g) was added dropwise over 10 minutes, keeping the reaction temperature below 10°C. The mixture was stirred continuously for 2 hours under these conditions. After the initial reaction period, the flask was removed from the ice bath, and 46 mL of distilled water was added dropwise over 15 minutes, allowing the temperature to gradually increase to 98°C. Additional warm distilled water (<50°C) was added, and the mixture was stirred for another 60 minutes. The reaction ended when 12 mL of 30% hydrogen peroxide solution (H_2O_2) was added to the mixture which then received 30 minutes of stirring to eliminate any remaining permanganate. The mixture was split into two equal parts, and each received 150 mL of distilled water. The suspensions were left undisturbed for 24 hours to allow

precipitation. The supernatant was decanted, and the solid product was washed once with 10% hydrochloric acid (HCl, 30 mL) and then five times with deionized water (30 mL each) until the pH reached neutrality (pH = 7). Finally, the product was dried at 60–70 °C to obtain nano graphene oxide. See Figure 1.

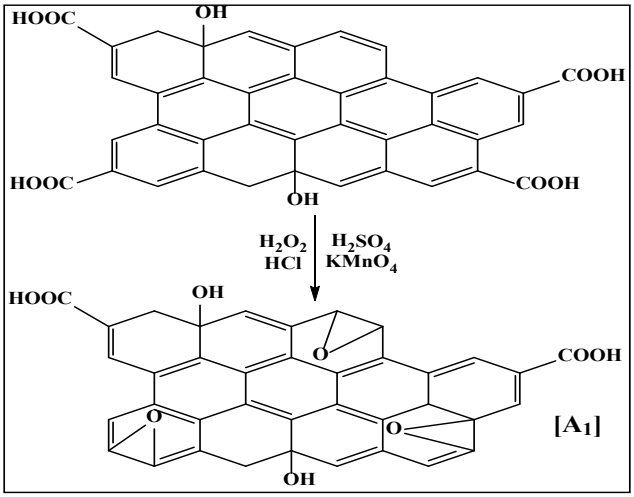

Fig. 1. Schematic illustration of the preparation process of nano-graphene oxide (nGO).

2.4 Synthesis of Azo dye derived from 2-amino-5-bromo-1,3,4-thiadiazole and vanillin

The targeted azo dye was synthesized through a two-step method to create the target azo dye by first diazotizing 2-amino-5-bromo-1,3,4-thiadiazole followed by vanillin coupling under alkaline conditions. In the first stage, 10 mmol of 2-amino-5-bromo-1,3,4-thiadiazole was dissolved in 20–30 mL of diluted hydrochloric acid (2–3 M) under constant stirring in an ice bath at temperatures between 0 and 5°C until a homogenous solution was obtained. Separately, a solution of sodium nitrite (12 mmol) in 10–15 mL of ice-cold distilled water was added dropwise to the cold acidic amine solution while stirring vigorously for 10–15 minutes at temperatures below 5°C. Excess nitrite was monitored using starch iodide paper or nitrite indicator strips, and the mixture was stirred for an additional hour at 0–5°C to complete the formation of the diazonium salt. In the second step, the newly prepared diazonium solution was slowly introduced into a chilled alkaline vanillin solution (10–12 mmol) at 0–5°C, with continuous stirring. The pH of the reaction medium was carefully maintained between 9 and 10 using dilute sodium hydroxide. The reaction mixture was stirred for 1 to 2 hours at a temperature between 0 and 5°C, then allowed to gradually reach room temperature over the hour. During this time, a precipitate of a characteristic color formed, confirming the conjugation reaction of the azo dye. The resulting solid product was collected by vacuum filtration and thoroughly washed with cold water and a small amount of cold ethanol to remove inorganic salts and unreacted vanillin, and subsequently purified by recrystallization of the ethanol-water mixture. The purified azo dye was dried under reduced pressure at a temperature between 40 and 50°C until a constant weight was achieved, yielding 85% of the final product. See Figure 2.

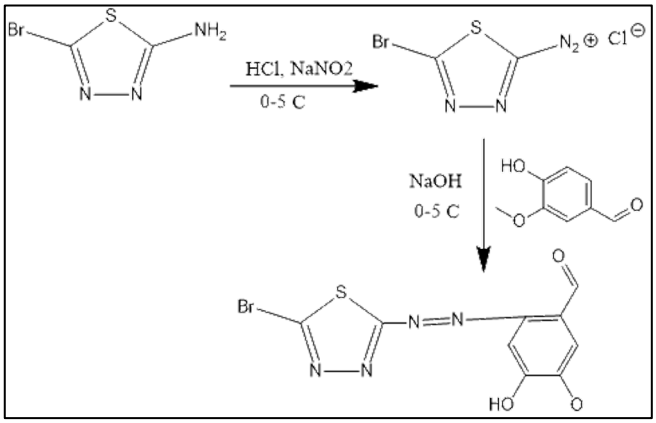

Fig. 2. Shows the synthesis pathway of an azo dye which results from combining 2-amino-5-bromo-1,3,4-thiadiazole with vanillin.

3 Results and discussion

3.1 Characterization

The SEM image displays graphene oxide nanoparticles through their thin stacked structures, which appear as wrinkled sheet-like materials with irregular uneven borders. The graphene oxide structure develops from graphite exfoliation while oxygen functional groups, including hydroxyl, carboxyl, and epoxy groups, integrate into the material. The graphene layers become non-uniform because of functional group incorporation, which results in the formation of ripples and wrinkles throughout the material. The surface corrugation pattern, which appears on the material surface, creates additional active sites for adsorption while increasing the material's accessible surface area. The particular structure of graphene oxide nanoparticles shows their successful conversion from graphite and their strong ability to adsorb substances. The porous layered structure of graphene oxide nanoparticles allows them to strongly interact with pollutants, which makes them suitable for environmental cleanup applications, as shown in Figure 3.

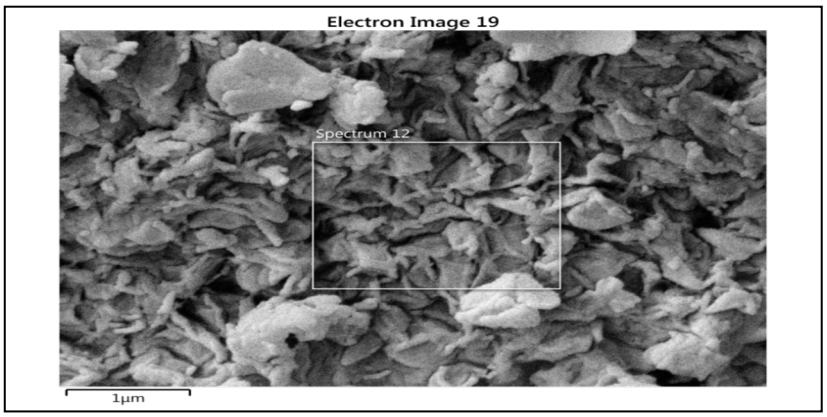

Fig. 3. Scanning electron microscope image (SEM) of graphene oxide nanoparticles.

The energy-dispersive X-ray spectroscopy (EDS) spectrum of the sample shows two main elements, which are carbon (C) and oxygen (O), at weight percentages of C = 66.3% and O = 33.7%, thus confirming the expected graphene oxide composition. The high oxygen content in this result proves that graphene oxide contains functional groups (hydroxyl, carboxyl, and epoxy) that formed during oxidation. The gold (Au) peaks in the spectrum stem from the thin gold coating used for SEM/EDS measurements, but they do not affect the material composition. The carbon-to-oxygen ratio (C/O ratio) serves as a vital metric to evaluate oxidation levels because increased oxygen content leads to more active surface sites. The SEM image showed wrinkled layered structures, which created a large surface area. The EDS results confirm that graphene oxide nanoparticles were successfully produced for their role as environmental pollution adsorbents. See Figure 4.

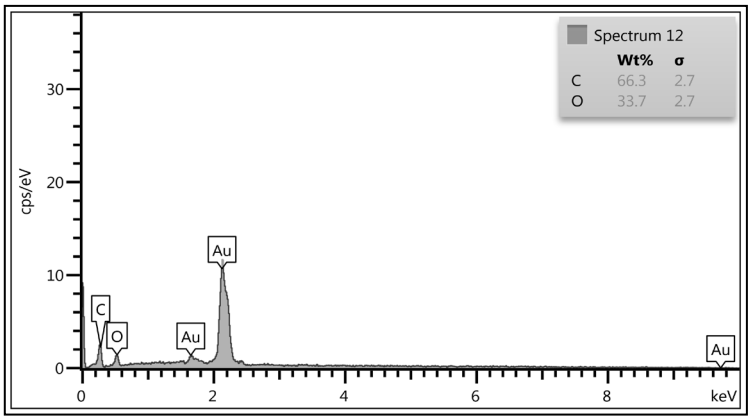

Fig. 4. The proportions of elements in the blocked absorbing surface GO.

X-ray diffraction (XRD) was employed to analyze graphene oxide crystallite structure and determine its interlayer distance. The diffraction pattern showed a distinct (001) reflection at $2\theta \approx 12°$, which indicated an interlayer distance of $d \approx 7.38$ Å. The increased spacing between layers indicates that the oxidation process was successful and oxygen groups formed between the graphene sheets. The (002) peak appeared at $2\theta \approx 26.6°$ with $d \approx 3.34$ Å spacing, which indicates the presence of unmodified graphitic structures. The material shows structural ordering through its multiple diffraction peaks, which include (100), (101/102), and (004) reflections. The surface analysis results from SEM, AFM, and EDS studies confirm the existence of two distinct phases in the material, which includes oxidized graphene oxide layers and graphitic regions.

To minimize re-accumulation and enhance the surface properties of graphene oxide for adsorption applications, it is recommended to optimize the washing methods and carefully control the reduction and drying conditions. See Figure 5.

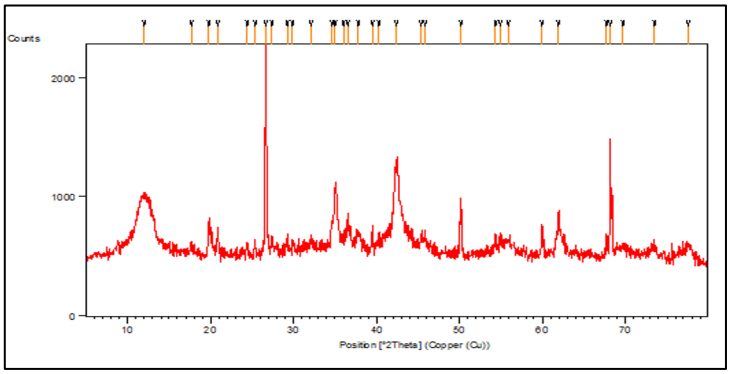

Fig. 5. The proportions of GO elements.

The atomic force microscopy (AFM) images display the nanoscale surface features of graphene oxide nanoparticles. The nanosheets display a flat, thin structure with localized wrinkles and height variations because oxygen-containing functional groups create disruptions in the regular graphene layer stacking. The AFM images show sheet thicknesses between (1–2) nm for single layers and higher values for multilayered structures which confirms the successful synthesis of few-layer graphene oxide. The surface shows a significant level of roughness which indicates an elevated number of active surface sites that are crucial for better adsorption performance and environmental applications. See Table 1, and Figure 6 a-c.

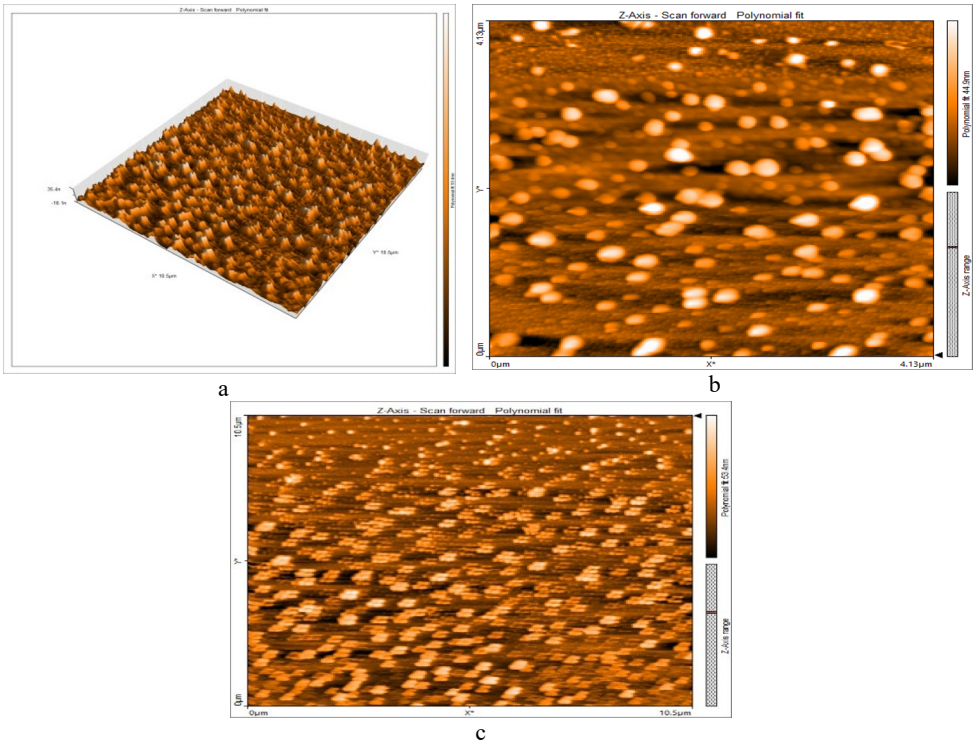

Fig. 6. The images of the nanocomposite under study by atomic force microscopy, (a) 3D-view, (b,c) 2D-view.

Table 1. Comparative summary of structural, morphological, and compositional characteristics of graphene oxide (GO).

Technique	Parameter Measured	Value / Observation	Interpretation
SEM	Morphology	Thin, wrinkled, stacked sheets with irregular edges	Wrinkles increase surface area and create abundant adsorption sites
SEM	Approximate lateral sheet size	200–800 nm (estimated from micrograph field)	Indicates nanosheet formation rather than bulk graphite
EDS	C/O ratio	C ≈ 66.3%, O ≈ 33.7% → C/O ≈ 1.96	Confirms oxidation and presence of –OH, –COOH, and epoxy groups
XRD	Crystallite size (Scherrer)	~25–35 nm	Indicates partial ordering and nanoscale domain size
XRD	Interlayer spacing (d_{001})	~7.38 Å	Expansion confirms successful oxidation of graphite to GO
AFM	Sheet thickness	1–2 nm (single layer), higher for multilayers	Confirms formation of few-layer GO
AFM	Surface roughness (Rq)	High roughness (qualitative)	Wrinkled topology enhances adsorption activity

3.2 Effect of different factors on adsorption efficiency for the removal of 2-(5-bromo-1,3,4-thiadiazol-2-yl)diazinyl-4-hydroxy-5-(λ¹-oxydanyl)benzaldehyde (V)

3.2.1 Effect of contact time

The equilibrium time (V) of dye adsorption was investigated by performing batch adsorption experiments at 298 K, using an initial dye concentration of 50 ppm and different contact times (1, 5, 20, and 30 minutes). A constant dose of 0.03 g of graphene oxide (GO) was used throughout the experiments. The results obtained, summarized in Table 1, were used to plot the adsorption capacity (q_e) versus contact time (t) of dye adsorption onto graphene oxide, as shown in Figure 7.

The adsorption pattern shows a gradual increase in adsorption capacity (q_e) with increasing contact time, indicating a rapid initial adsorption rate due to the abundance of active sites on the graphene oxide surface. Equilibrium was achieved at 30 minutes, and no significant increase in adsorption capacity was observed thereafter. This behavior indicates the saturation of the active sites and the dye molecules reaching a state of dynamic equilibrium between the solution and the surface of the absorbent material. This observed trend confirms the efficiency and speed of the adsorption of graphene oxide nanoparticles towards the dye (V).

Table 1. Demonstrates the effects of contact time on adsorption capacity at 25°C and an initial dye concentration of 50 ppm.

T (min)	qe(mg/L)
1	28.2
5	29.4
10 15	30.6 31.5 31.8
20 25	31.9
30	32

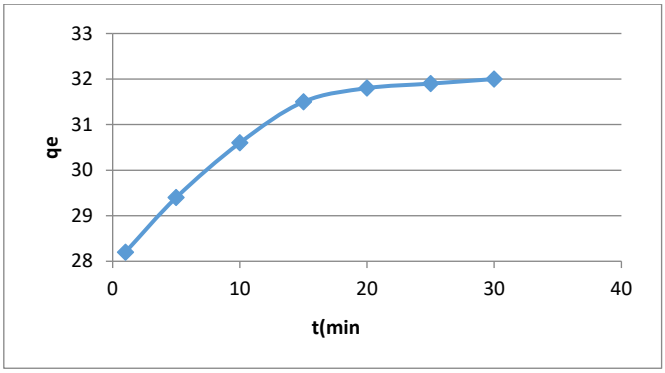

Fig. 7. Effect of contact time on adsorption performance of graphene oxide at 25 °C using an initial dye concentration of 50 ppm.

3.2.2 Effect of adsorbent dosage

The effect of adsorbent dosage on the adsorption of dye (V) was investigated using graphene oxide (GO) nanoparticles at a constant initial dye concentration and a temperature of 298 K. The results, summarized in Table 2 and illustrated in Figure 8, demonstrate the effect of varying graphene oxide concentrations on the adsorption capacity. The amount of dye (V) adsorption reached its maximum at 0.03 g of GO when the adsorbent dosage was increased. The adsorption process did not show any additional improvement when the GO dosage exceeded this point because all available active sites on the surface became fully occupied. The highest adsorption efficiency occurred when the adsorbent dosage reached this particular value under the studied conditions.

Table 2. Effect of adsorbent dosage.

The Absorbent Surface	M(g)	C_o (ppm)	Qe (mg/L)
GO	0.01	50	14
	0.03	50	25.4
	0.05	50	5.2

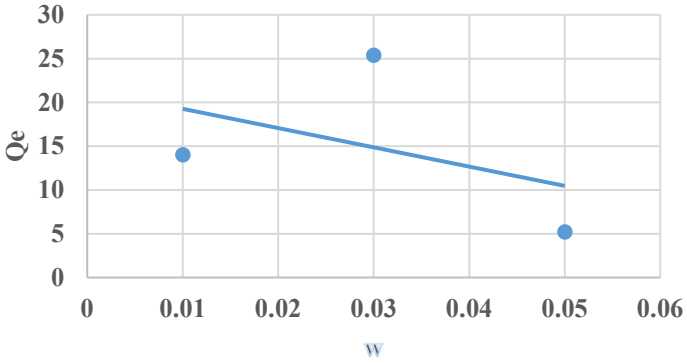

Fig. 8. Effect of adsorbent dosage.

3.2.3 Effect of initial concentration and temperature on the adsorption process

The effect of the initial dye concentration and solution temperature on the dye adsorption (V) onto graphene oxide (GO) nanoparticles was systematically investigated. The adsorption capacity (q_e) was analyzed as a function of the equilibrium dye concentration (C_e), and the resulting adsorption equations are shown in Figure 9. The experimental data showed that dye absorption rates increased with rising dye concentrations because elevated dye concentrations created additional binding sites for dye molecules. The adsorption process became less effective when the solution temperature increased, which indicates that adsorption follows an exothermic reaction pattern. The research data demonstrates how temperature affects adsorption reactions while showing that dye molecules maintain strong bonding with GO surfaces from start to finish of the experiment. This behavior can be explained by the release of heat energy during the formation of internal molecular bonds (as reported in the literature) as well as the formation of physical or chemical interactions between the dye molecules and the adsorbent surface.

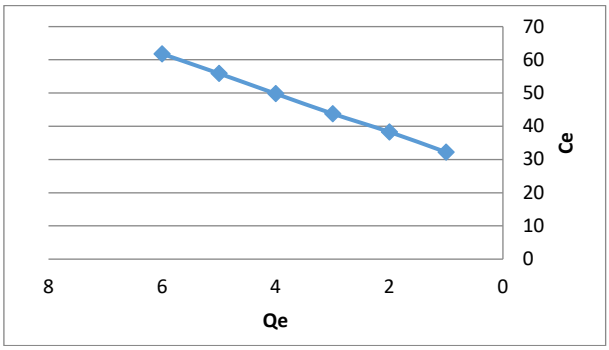

(a)

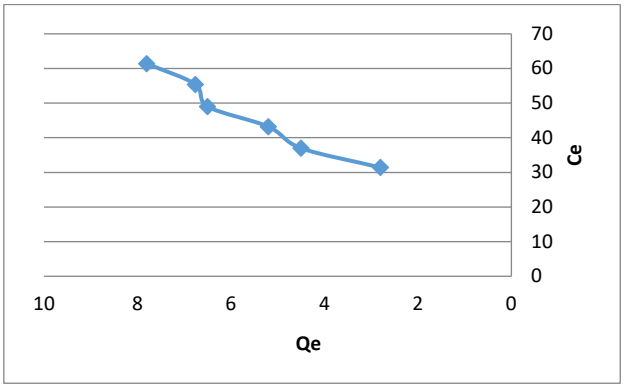
70
60
50
40
30
20
10
0
Ce
10
8
6
4
2
0
Qe

(b)

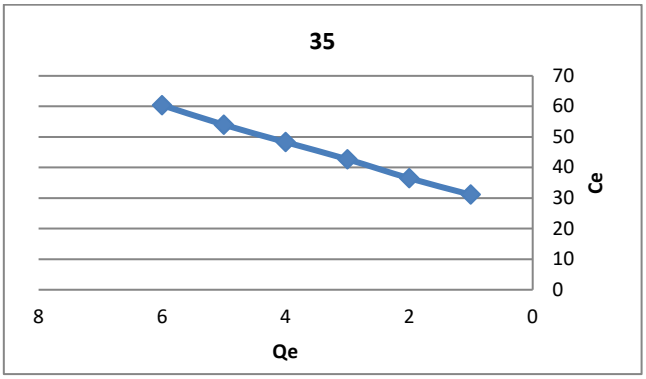
35
70
60
50
40
30
20
10
0
Ce
8
6
4
2
0
Qe

(C)

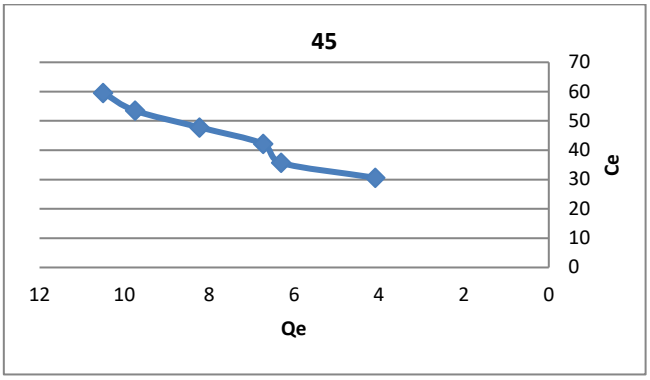
45
70
60
50
40
30
20
10
0
Ce
12
10
8
6
4
2
0
Qe

(d)

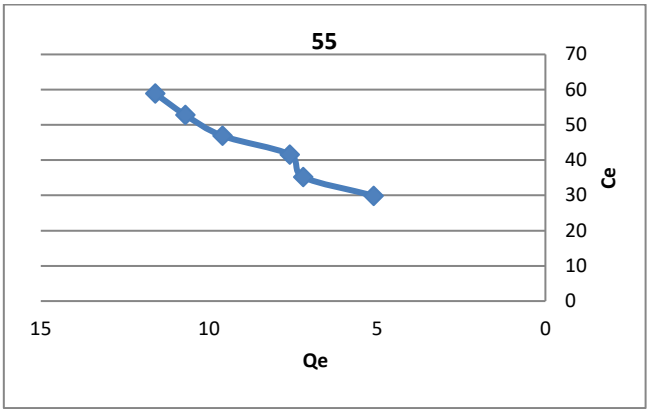

(e)

Fig. 9. Adsorption curves showing the relationship between the concentration of the residual dye and the adsorption capacity of graphene oxide at different temperatures: (a) 288 K, (b) 298 K, (c) 308 K, (d) 318 K, and (e) 328 K.

3.3 Adsorption kinetics

3.3.1 Pseudo-first-order kinetic model

The linear form of the first-order semi-kinetic equation was used to determine the rate constants and correlation coefficients for dye adsorption (V) on the surface of graphene oxide (GO) nanoparticles. Table 3 summarizes the calculated rate constants. A significant discrepancy was observed between the experimentally determined adsorption amplitudes and the values predicted by the first-order semi-kinetic model across all studied temperatures. The pseudo-first-order kinetic model fails to accurately describe the dye (V) adsorption process onto GO nanoparticles because of this observed discrepancy, as shown in Figure 10, Figure 11, and Figure 12.

Table 3. The calculated rate constant values for the pseudo-first order model.

Time	Ln (Qe-Qt)
1	1.3
5	1
10	0.26
15	-0.105

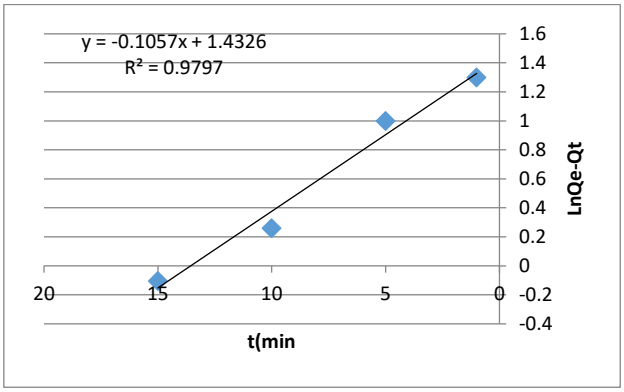

Fig. 10. The pseudo-first-order kinetic diagrams of dye absorption (V) on graphene oxide at different temperatures.

3.3.2 Pseudo-second-order kinetic model

The linear form of the pseudo-second-order kinetic equation was applied to calculate rate constants and R^2 values for V dye adsorption onto GO nanoparticles through linearized model analysis. The pseudo-second-order model produced higher correlation coefficients than the pseudo-first-order model, according to Table 4 results. The pseudo-second-order model predicted adsorption capacities that matched experimental results better than the pseudo-first-order model at all investigated temperatures. The pseudo-second-order model rate constants (K_2) exceeded the pseudo-first-order model rate constants (K_1) at every temperature point. The pseudo-second-order kinetic model demonstrates superior ability to explain the dye (V) adsorption process onto GO nanoparticles.

Table 4. Pseudo-Second-Order Kinetic Model for MB adsorption onto the adsorbent surface at different temperatures.

Time	**t/q_t**
1	0.035
5	0.17
10	0.32
15	0.47

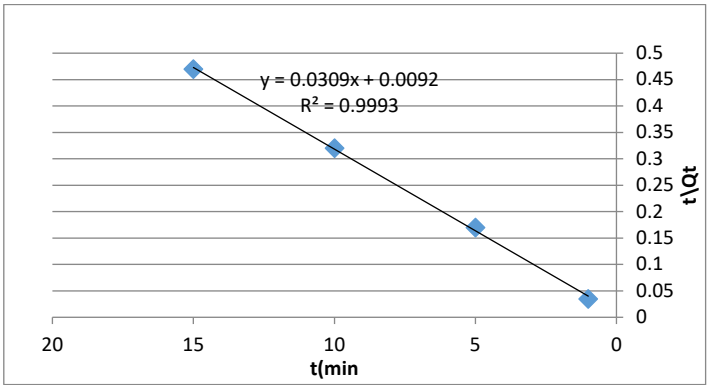

Fig. 11. The pseudo-second-order kinetic diagrams of dye absorption (V) onto the adsorbent surface at different temperatures.

3.4 Langmuir isotherm model

The linearized form of the Langmuir equation was applied to the experimental data for the adsorption of dye (V) onto graphene oxide (GO) nanoparticles at different temperatures (288, 298, 308, 318, and 328 K). The Langmuir constants were determined from the slope and intercept of the linear plot of (Ce/qe) versus Ce

The Langmuir constants obtained from Table 5 show that GO adsorption capacity for dye (V) grows when the temperature increases. The experimental data shows excellent agreement with the Langmuir isotherm model because the correlation coefficient ($R^2 = 0.9372$) indicates a good fit.

The adsorption data was analyzed through Equation (1) at different temperatures to obtain the isotherm parameters, which are presented in Table 5. The Langmuir model successfully explains how dye (V) adsorption onto graphene oxide surfaces occurs during the studied experimental conditions. The corresponding isotherm results are presented in Table (5).

$$\frac{Ce}{Qe} = \frac{1}{QmaxKL} + \frac{Ce}{Qmax} \quad \text{…….. equation (1)}$$

Where:

C e : is the equilibrium concentration.

Q e : is the amount of adsorbate adsorbed at equilibrium.

Q max : is the maximum monolayer adsorption capacity.

K L: is the Langmuir constant.

Table 5. Adsorption data for methylene blue (MB) on graphene oxide (GO) at different temperatures were fitted using the Langmuir isothermal model.

The Absorbent Surface	**Temperature (K)**	R^2	Qe_{max}	K_L
GO	288	0.922	71.4	0.356
	298	0.7021	142.8	0.0885
	308	0.7268	101	0.0912
	318	0.5306	142.8	0.494
	328	0.3972	303	0.0204

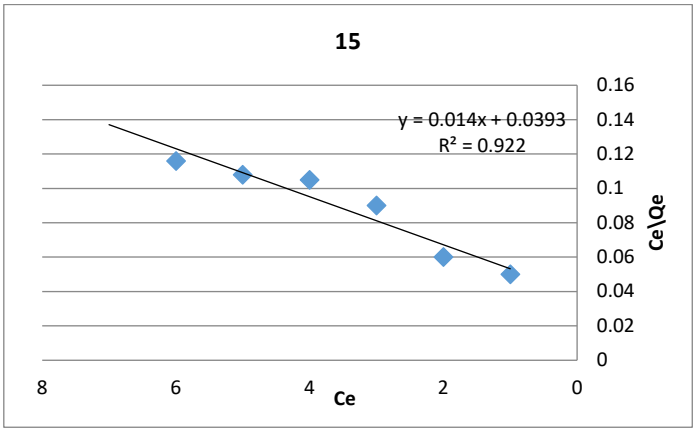

(a)

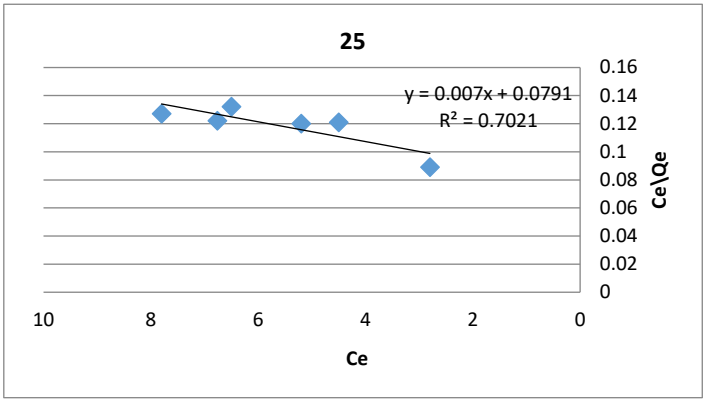

(b)

Fig. 12. The adsorption data for the dye (V) on graphene oxide (GO) at different temperatures were fitted using the Langmuir isothermal model: (a) 288 K, (b) 298 K.

3.5 Freundlich isotherm model

The linear form of the Freundlich thermometric equation was applied to evaluate the adsorption of dye (V) onto graphene oxide (GO) at different temperatures. The Freundlich constants were determined from the slope and intersection of the linear curve by plotting q_e versus ln C_e , as shown in Figure 13. As summarized in Table 6, the Freundlich constant

showed a decrease with rising temperatures, which indicates GO has lower affinity for dye (V) adsorption at elevated temperatures. The observed trend supports the exothermic nature of the adsorption process, which matches findings from previous research. The Freundlich isotherm model shows an excellent fit to the adsorption system because the average correlation coefficient (R^2 = 0.9372) indicates a good match between experimental data and model predictions.

Equation (4) was applied to analyze the absorption of methylene blue (MB) on the surface of graphene oxide (GO) at different temperatures. The resulting data were plotted, and the corresponding results are summarized in Table 6.

$$\ln Qe = \ln Kf + \frac{1}{n}\ln Ce \quad \text{..... equation (2)}$$

where:

Qe: The amount of adsorbed substance absorbed at equilibrium per unit mass of adsorbent (mg/g).
Ce: The concentration of adsorbed substance at equilibrium in the solution (mg/L).
Kf: Freundlich's adsorption constant, representing the adsorption capacity.
1/n: The heterogeneity factor, reflecting the intensity of adsorption or surface heterogeneity.

Table 6. Adsorption data of (V) dye on GO at different temperatures fitted by the Freundlich isotherm model.

The Absorbent Surface	Temperature (K)	R^2	n	K_f
GO	288	0.968	2.345	8.782
	298	0.8947	1.506	7.305
	308	0.9523	1.643	7.259
	318	0.9458	1.433	6.508
	328	0.9801	1.140	5.131

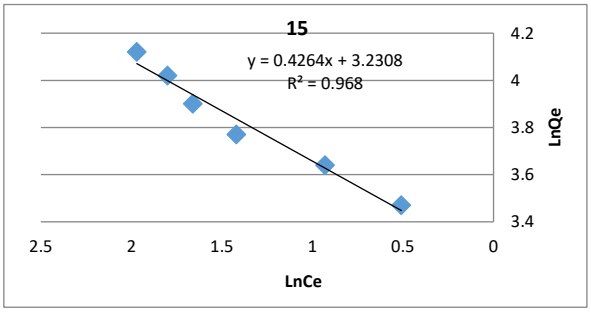

(a)

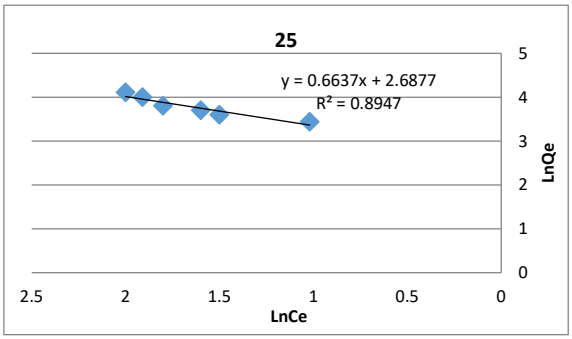

(b)

Fig. 13. Adsorption data of dye (V) on graphene oxide (GO) fitted using the Freundlich isotherm model at different temperatures: (a) 288 K and (b) 298 K.

4 Conclusion

Synthetic dyes represent a major class of water pollutants due to their high chemical stability and resistance to degradation, posing significant environmental and public health risks. In this study, a novel azo dye was successfully synthesized and structurally characterized using various spectroscopic techniques. Its removal from aqueous solutions was investigated using graphene oxide (GO) nanoparticles as an effective adsorbent. The adsorption process on the graphene oxide surface was found to be exothermic, as evidenced by its increased adsorption

capacity at low temperatures. Kinetic analysis revealed that the quasi-second-order model best suited the experimental data, indicating that chemisorption is the dominant mechanism. Furthermore, the equilibrium data showed good agreement with the Langmuir and Freundlich isothermal models, with high correlation coefficients. The slightly higher R^2 value of the Freundlich model suggests that adsorption often occurs on a heterogeneous surface, consistent with the uneven distribution of oxygen-containing functional groups on graphene oxide. Morphological analysis using scanning electron microscopy confirmed that graphene oxide has a wrinkled, layered, and heterogeneous surface structure with a high surface area, which enhances dye adsorption. Overall, the high removal efficiency achieved in this study demonstrates that graphene oxide nanoparticles are a promising adsorbent material for wastewater treatment and the effective removal of dye pollutants.

References

1. Mishra, D. P.; Sahu, P. K.; Acharya, B.; Mishra, S. P.; Bhati, S. A Review of the Synthesis and Application of Azo Dyes and Metal Complexes for Emerging Antimicrobial Therapies. *Results Chem.* (2024), **10**, 101712.
2. Benkhaya, S.; M'rabet, S.; El Harfi, A. Classifications, Properties, Recent Synthesis and Applications of Azo Dyes. *Heliyon* (2020), **6** (1).
3. Shabir, G.; Su, J.; Saeed, A.; Ul-Hamid, A. New Heterocyclic Azo Dyes: Design, Synthesis, and Application on Leather. *Fiber Polym.* (2021), **22** (12), 3385–3392.
4. Singh, G. B.; Vinayak, A.; Mudgal, G.; Kesari, K. K. Azo Dye Bioremediation: An Interdisciplinary Path to Sustainable Fashion. *Environ. Technol. Innov.* (2024), **36**, 103832.
5. Chowdhury, A. P.; Anantharaju, K. S.; Keshavamurthy, K.; Rokhum, S. L. Recent Advances in Efficient Photocatalytic Degradation Approaches for Azo Dyes. *J. Chem.* (2023), 2023.
6. Emanuele, L.; D'Auria, M. The Use of Heterocyclic Azo Dyes on Different Textile Materials: A Review. *Organics* (2024), **5** (3), 277–289.
7. Ansar, A.; Du, J.; Javed, Q.; Adnan, M.; Javaid, I. Biodegradable Waste in Compost Production: A Review of Its Economic Potential. *Nitrogen* (2025), **6** (2).
8. Selvaraj, V.; Karthika, T. S.; Mansiya, C.; Alagar, M. An Over Review on Recently Developed Techniques, Mechanisms and Intermediates Involved in the Advanced Azo Dye Degradation for Industrial Applications. *J. Mol. Struct.* (2021), **1224**, 129195.
9. Liu, Z.; Zheng, Z.; Liu, Y.; Yang, X.; Chen, Y.; Tan, F. Autonomous Self-Propelled Reduced Graphene Oxide Hydrogel-CuO@rGO Micromotors for High-Efficiency Removal of Organic Dye Pollutant. *J. Contam. Hydrol.* (2025), **274**, 104650.
10. Naseer, M.; Nazir, S.; Kausar, A.; Rashid, M. A.; Usman, M.; Naseer, R.; Iqbal, J. Enhanced Removal of Cationic Dyes Using Copper-Based MOF–Graphene Oxide Composite: Synthesis, Characterization and Performance Evaluation. *Chem. Eng. Sci.* (2025), **307**, 121362.
11. Ibrahim, A. A. Microwave-Assisted Biogenic Synthesis of Pure Copper Oxide Nanoparticles by *Lepidium sativum* L. Leaves Extract: Characterization and Evaluation of Antibacterial Activity. *J. Biotechnol.* (2025), **406**, 82–90.
12. Sagadevan, S.; Lett, J. A.; Weldegebrieal, G. K.; Garg, S.; Oh, W. C.; Hamizi, N. A.; Johan, M. R. Enhanced Photocatalytic Activity of rGO–CuO Nanocomposites for the Degradation of Organic Pollutants. *Catalysts* (2021), **11** (8).

13. Liu, Z.; Zheng, Z.; Liu, Y.; Yang, X.; Chen, Y.; Tan, F. Autonomous Self-Propelled Reduced Graphene Oxide Hydrogel-CuO@rGO Micromotors for High-Efficiency Removal of Organic Dye Pollutant. *J. Contam. Hydrol.* (2025), **274**, 104650. (duplicate entry)
14. Carr, A. J.; Lee, S. E.; Uysal, A. Ion and Water Adsorption to Graphene and Graphene Oxide Surfaces. *Nanoscale* (2023), **15** (35), 14319–14337.
15. Al-Odayni, A.-B.; Alsubaie, F. S.; Saeed, W. S. Nitrogen-Rich Polyaniline-Based Activated Carbon for Water Treatment: Adsorption Kinetics of Anionic Dye Methyl Orange. *Polymers* (2023), **15** (4), 806.